Journal of Hydrology 564 (2018) 329–341

Contents lists available at ScienceDirect

Journal of Hydrology

journal homepage: www.elsevier.com/locate/jhydrol

Research papers

Morphological variability of the active Yellow River mouth under the new regime of riverine delivery

Hongyu Ji[a], Shenliang Chen[a,*], Shunqi Pan[b], Congliang Xu[c], Chao Jiang[a], Yaoshen Fan[a]

[a] State Key Laboratory of Estuarine and Coastal Research, East China Normal University, Shanghai 200062, China
[b] Hydro-Environmental Research Centre, School of Engineering, Cardiff University, Cardiff CF24 3AA, UK
[c] Institute of the Yellow River Estuary and Coast Science, Dongying 257000, Shandong, China

ARTICLE INFO

This manuscript was handled by A. Bardossy, Editor-in-Chief, with the assistance of Jozsef Szilagyi, Associate Editor

Keywords:
Active Yellow River mouth
New regime of WSRS
Morphological variability
Accretion and erosion
Human interference

ABSTRACT

The Yellow River subaqueous delta (YRSD), once the most rapid depo-center among river deltas worldwide, has been under the risks of subsidence and degradation due to the new regime of riverine delivery affected by human interventions. Utilizing hydrologic and bathymetric surveying datasets, we examined the latest regime of river input from the perspective of water-sediment relationship, and the responding morphological evolutionary processes of active YRSD over a period of 20 years between 1996 and 2016. Results show that the new discharge regime is strongly interfered by the Water-Sediment Regulation Scheme (WSRS), characterized by a more drastic decline of sediment load than that of water discharge; more harmonious relationship between water and sediment discharges in the lower reach of the river to the sea; coarser sediment delivery and low suspended sediment concentration (SSC). We identified inverse erosion-accretion trends in the subaqueous region: net accretion of 0.15 m/yr in the active Yellow River mouth (AYRM) and severe erosion of −0.1 m/yr in the Gudong littoral zone (GDLZ). As the primary sink for sediment delivery, AYRM received approximately 68% of sediment delivery during the study period and sedimentation was mainly occurred in the shallower area where water depth was less than 10 m. In addition, recent morphological evolution of AYRM is found to have undergone through four stages, namely: moderate accretion (1996–2002), rapid accretion (2002–2007), reduced accretion (2007–2015) and rapid erosion (2015–2016). The new regime of riverine delivery presents multiple spatiotemporal scales in shaping deltaic morphology. Compared with the previous research, we present the morphological evolution of deltaic system over decadal timescale is strongly influenced by reduction of sediment supply derived from basin-scale human impacts, and the variability of subaqueous portion during the study period is closely related to inter-annual variability of river input. Besides, the building of AYRM is shaped by event-scale WSRS induced-floodwater, and decade-scale change of sediment pathway governed by frequent mouth channel migration. The results show, for the first time, that AYRM has experienced a significant erosion since the implementation of WSRS, with a decline of 99% sediment delivery in 2016 compared to the natural mode during 1950s. The results also indicate that to maintain the erosion-accretion balance of AYRM, an estimation of 41.4–62.3 Mt/yr sediment delivery should be kept. Due to the fluvial regime change from the natural to the highly human-regulated modes, the AYRM, as well as the whole YRSD, is expected to be transforming from the accretion to erosion states.

1. Introduction

Due to naturalflat terrain, fertile soils and abundant water resources, over half a billion people densely inhabited in river deltas during the Anthropocene (Syvitski et al., 2009; Kuenzer et al., 2014). With rapid population and economic growth over the last century, anthropogenic interventions drastically intensified in river basins. Upstream damming, flow diversion, and intensified water consumption in river catchment dominated the reduction of river input in recent decades (Sanchez-Arcilla et al., 1998; Carriquiry and Sánchez, 1999; Vörösmarty et al., 2003; Walling, 2006). As a result, river deltas today are facing increasing challenges in stabilizing deltaic morphology and shoreline. As there have been severe coastal land loss in Mississippi delta and Nile delta (Stanley, 1996; Blum and Roberts, 2009), large-scale shoreline retreat in Mekong delta (Anthony et al., 2015), recession and land subsidence in Yangtze delta (Yang et al., 2011a) and transformation from accretion to erosion in Pearl River delta (Dai et al., 2008; Wu et al., 2016). Therefore, scientists and engineers have

* Corresponding author.
E-mail address: slchen@sklec.ecnu.cn (S. Chen).

https://doi.org/10.1016/j.jhydrol.2018.07.014
Received 1 June 2018; Received in revised form 4 July 2018; Accepted 7 July 2018
Available online 09 July 2018

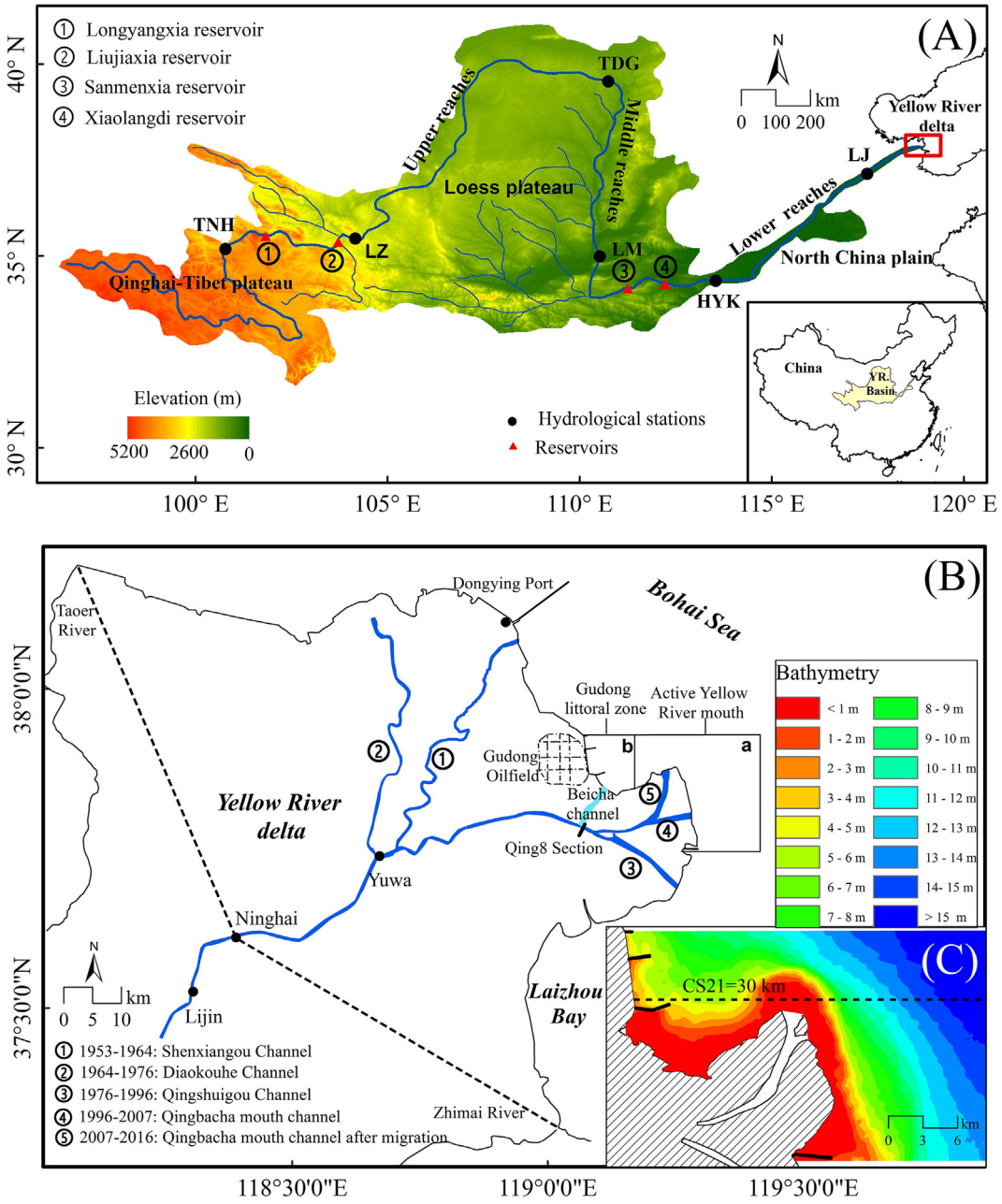

Fig. 1. Sketch maps of Yellow River catchment and Yellow River delta. (A) Yellow River drainage basin, where black dots represent the key hydrological stations (Tangnaihai (TNH), Lanzhou (LZ), Toudaoguai (TDG), Longmen (LM), Huayuankou (HYK), Lijin (LJ)), red triangles represent large reservoirs in the Yellow River basin; (B) Modern Yellow River delta. The map is projected to UTM Zone 50 N in WGS84 datum with central meridian 117°E; Study area of AYRM (study area a) and GDLZ (study area b), are separated by the straight line (37.80°N, 119.18°E), (37.91°N.119.18°E); The latest channel migration occurred in artificial diversion at Qing 8 section (1996) and natural shifts (2007) of Qingbacha mouth channel; (C) Bathymetry of active YRSD. (For interpretation of the references to colour in this figure legend, the reader is referred to the web version of this article.)

considerably expanded monitoring and impact studies on sustainability of river deltas (Giosan et al., 2014), which has made the latest regime of river input and responded geomorphic and environmental implications in worldwide river deltas a hotspot in hydrologic and coastal research.

Similar to other megadeltas, morphologic evolution of Yellow River (Huanghe) delta is significantly impacted by human activities. Intensified human intervention in the river catchment induced sharp decline in river input in recent years (Wang et al., 2006a, 2007; Syvitski and Saito, 2007; Miao et al., 2011; Liu et al., 2012). In addition, there are extensive engineering activities influencing the development of delta, such as human-avulsion engineering projects for oilfield protection, dikes and levees for flood control, groynes and breakwaters for storm surge defense and coastal protection (Bi et al., 2014; Zheng et al., 2018). Other economic activities including oil exploiting, land reclamation and aquaculture are rapidly developing, which also have profound impacts for ecosystem vulnerability and landscape change (Yue et al., 2003; Zhang et al., 2017; Chi et al., 2018; Fan et al., 2018a). Thus, it is urgent for investigations to be carried out to maintain the delta sustainability by keeping the right balance between human intervention and natural forcing.

On the other hand, Yellow River delta is distinctive from other megadeltas with its developing pattern. The delta has been formed as a fan-shaped landscape with frequent deltaic channel avulsions since 1855; Until 2016, there have been 11 major channel avulsions and

frequent channel bifurcations (Zheng et al., 2018). Thereafter, the Yellow River delta has high spatial variations in evolutionary processes: rapid-accretion occurring in active Yellow River mouth (AYRM) with sufficient sediment supply and erosion in abandoned river mouth due to sediment starvation (Li et al., 2000; Chu et al., 2006; Cui and Li, 2011; Xing et al., 2016). Multi-year estimation indicates that the sediment delivered to the delta annually is in the range of 1.08 billion tons (Milliman and Meade, 1983), which makes it one of the most rapid deposition center in the world (Zhou et al., 2015). However, associated with the reduction of river input in recent decades, the aggradation rates of AYRM has slowed down, especially after 1996 when the channel artificial diversion at Qing 8 section (Cui and Li, 2011; Jiang et al., 2017; Wu et al., 2017). In addition, the implementation of Water-Sediment Regulation Scheme (WSRS) since 2002 has transformed the river discharge to a highly human-altered regime: the natural seasonal variability of river discharge being overridden by the prior designed short-term substantial river discharge delivery. Fourteen years after the operation of this basin-scale water regulation program, it is perhaps the time to re-estimate the new regime of human activity-derived riverine delivery and consequent changes in coastal environment in Yellow River delta.

Numerous studies have been conducted in the primary role of WSRS in promoting the spread of nutrients (Wang et al., 2017b), reshaping shoreline dynamics (Cui and Li, 2011; Kong et al., 2015a; Fan et al., 2018b), changing land areas in subaerial delta (Xu, 2008; Bi et al., 2014; Jiang et al., 2017; Wu et al., 2017) and dominating evolution processes of active Yellow River subaqueous delta (YRSD). Specifically, Bi et al. (2014) found the profile slope of subaqueous delta increasing as delta advancing seaward near the active river mouth. Wu et al. (2017) considered the grain size of sediment delivery and reduction of river input as dominated factors driving morphological evolution in YRSD since the operation of WSRS. However, under recent man-derived fluvial regime, little is known about morphological adaption in the deposition area of WSRS-delivered sediment suggested by Wang et al. (2017a). In addition, the spatial variability of active YRSD have been frequently ignored due to the lack of high-resolution geometric survey data. As the key element of land-ocean interaction processes, the active YRSD behavior to the altered fluvial regime needs further appreciation and evaluation.

Thus in this study, the variation of AYRM under the new regime of river input is examined, based on high-resolution bathymetric survey data in active YRSD from 1996 to 2016 and temporal changes in water and sediment delivery. We first define the new regime of terrestrial delivery by comparing it with the previous river input from the point of statistical analysis. Then we analyze the different erosion-accretion patterns in active YRSD, including AYRM and Gudong littoral zone (GDLZ), and quantify. Finally, we discuss the dominant factors of new discharge regime impacts on the deltaic behavior, and provide recommendations for the Yellow River management from the perspective of deltaic sedimentation system, based on the better understanding of the recent morphologic variability corresponding to the human-altered discharge regime gained from this study.

2. Regional setting

The Yellow River originates from Qinghai-Tibet Plateau and runs through Loess Plateau and North China Plain successively, finally emptying into the Bohai Sea, exceeding its length with 5464 km and a river catchment of 7.52×10^5 km^2 (Fig. 1A). The upper reach of the Yellow River is the main water source, providing more than 90% of total water discharge but small amount of sediment. Because of the intensive erosion in Loess Plateau, the middle reach becomes the primary source of suspended sediment, dominating over 90% of total sediment load in the river drainage (Miao et al., 2011). The lower reach channel is the sink of sediment from upstream, especially coarse sediment, for the gentle terrain and few tributaries. In addition, the riverbed of the lower reach is higher than the elevation of riverside and considered as “Hanging River”. There have been many flooding disasters in the lower reach drainage historically when peak flows bursting the riverbank during the flood season, causing severe losses in the alluvial plain of the lower Yellow River.

The modern Yellow River delta has begun to build out rapidly since the Yellow River breached at Tongwaxiang and shifted from Jiangsu Province to the Daqinghe River Course, entering into the Bohai Sea through Shandong Province (Chu et al., 2006). Deltaic channel shifted frequently at the apex of Ninghai before 1953 and then it moved downstream to Yuwa (Li et al., 2001; Peng et al., 2010). Since then, the deltaic channel followed by Shenxiangou channel (1953–1964), Diaokouhe channel (1964–1976), Qingshuigou channel (1976-present), then artificially shifted at the Qing 8 section in August 1996 as the present Qingbacha mouth channel (Fig. 1B), due to the concerns of the stability of Qingshuigou channel and decrease in the potential risk of flooding (Syvitski and Saito, 2007; Peng et al., 2010).

We divide the active YRSD into sub-regions of AYRM and GDLZ, according to different fluvial and marine dynamics and erosion-accretion trends (Fig. 1B). The evolution process of AYRM is determined by collective long-term erosion and short-term rapid accretion during flood season within a year, particularly after the implementation of WSRS. During WSRS (on average ~20 days each year), high concentration suspended sediment rapidly deposited within 10 m water depth in the river mouth, due to the barrier effect of the tidal shear front on the river-laden sediment dispersion (Bi et al., 2010; Wu et al., 2015). While in other days especially in winter, sediment resuspended mostly by storm waves and transported to offshore sea (Yang et al., 2011b). Gudong Oilfield is located in the northwest of AYRM (Fig. 1B), producing 30 million tons of oil per year (Ren and Walker, 1998). 17.2-km-long seawalls were constructed as relatively stable artificial coastline between 1985 and 1987 to protect the oilfield. However, there is huge spending every year to sustain the coastal protection near Gudong, but the deepest water depth near the seawall has exceeded 4.7 m by in-situ observation in 2016 (Fig. 1C).

The YRSD is dominated by irregular-semi diurnal tide with mean tidal range of 0.6–0.8 m near the river mouth (Li et al., 1998). Tidal current is parallel to the coast, which flows southward during flood tide and northward during ebb tide with the current speed of 1.0–2.0 m/s (Wang et al., 2010a). The residual current averages 0.2–0.3 m/s in surface layers, driven by monsoon winds and fluvial discharge (Zhang et al., 1990). Waves off the river mouth is generally driven by southerly winds in summer and northeasterly winds in winter with an average wave height up to 1.5 m, enhancing the resuspension of sediments in the littoral area of Yellow River delta, especially in Shenxiangou old estuary and Gudong nearshore (Chu et al., 2006). Sandy silt accounts for the largest proportion in seabed surface sediment type according to the classification of Folk (Ren et al., 2011).

3. Materials and methods

3.1. Data collection

We gathered monthly flow discharge, sediment load at Huayuankou and Lijin stations and annual median grain size at Lijin station from the Yellow River Conservancy Commission (YRCC). Sediment retention volume behind reservoirs/dams and sediment extraction in the lower reach area are available from Bulletin of Chinese River Sediment and Bulletin of Yellow River Sediment. Sediment retention by soil conservation practice is estimated from Gao et al. (2016). Since 1996, high-resolution subaqueous topography (spacing 250–1000 m) in AYRM was measured in 21, 41 or 81 transects. Different-period topography shared similar transection range, and was precisely measured by SDH-13D digital echo sounder. Satellite images were achieved by Earth Resources Observation and Science (EROS) Center (http://glovis.usgs.gov/). We extracted instantaneous waterline as deltaic shoreline from remote

Table 1
Detailed information of subaqueous transects and satellite images in corresponding period.

Date (month/year)	Number of subaqueous profiles	Intervals between subaqueous transects (m)	Coverage	Acquisition time of satellite images	Image type
09/1996	41	500	a&b	11/02/1997	TM
10/1998	41	500	a	10/09/1998	TM
06/2001	81	250	a&b	06/06/2001	ETM +
08/2002	81	250	a&b	28/08/2002	ETM +
08/2004	81	250	a&b	12/10/2004	TM
04/2007	21	1000	a&b	28/04/2007	TM
06/2011	41	500	a&b	02/06/2011	ETM +
08/2015	41	500	a&b	27/10/2015	OLI
10/2016	41	500	a&b	10/08/2016	OLI

sensing data of Landsat Multispectral Scanner (MSS), Landsat Thematic Mapper (TM), Landsat Enhanced Thematic Mapper (ETM +) and Operational Land Imager (OLI) satellite images during 1996–2016 (Table 1).

3.2. Methods

3.2.1. Trend test and abrupt change point analysis

We use non-parametric Mann-Kendall test in this study (Mann, 1945; Kendall, 1975), which has been widely used to examine varying trend in hydrological and meteorological time-series (Zhang et al., 2008; Zhao et al., 2008; Zhang et al., 2010; Dai et al., 2015), to detect the decreasing trends in Yellow River water and sediment delivery. A positive value of the standardized statistics Z indicates an upward varying trend and vice versa. The null hypothesis of no trend is rejected if Z greater than 1.96 at 0.05 significance level. And a bigger absolute value of Z is considered to reflect a stronger time-series variability. The Kendall slope β, for $\forall\, j > i$, is calculated as$\beta = \text{Median}\left(\frac{x_i - x_j}{i-j}\right)$, β is the median of all group pairs in the time-series sequence, an estimator of detecting the increasing/decreasing values with time. Detailed calculation processes can be referred to the article by Zhao et al. (2008).

The Pettitt test (Pettitt, 1979), which has been widely used in the detection significant change-point in the hydrologic time-series (Xie et al., 2013; Liu et al., 2014a; Zhao et al., 2014), is used in this study to detect the change-point in water and sediment delivery. Considering a sequence of random variables X_i (i = 1,2,…,T) and exists a change-point at τ if X_i for i = 1,…, τ has a common distribution function F_1 (X) and X_i for $i = \tau + 1,\ldots, T$ has a common distribution function F_2 (X) (F_1 (X) ≠ F_2 (X)). Propose for the test of H: no change against A: change by statistic: $K_T = \max_{1\leqslant i<T} |U_{t,T}|$, where $U_{t,T} = \sum_{i=1}^{t}\sum_{j=i+1}^{T} \text{sgn}(x_i - x_j)$, sgn($x$) = 1 if $x_i - x_j > 0$, 0 if $x_i - x_j = 0$, −1 if $x_i - x_j < 0$. The significance level for K_T is determined by $p = \exp\left(\frac{-6K_T^2}{T^3+T^2}\right)$. If $K_T = \max_{1\leqslant i<T} U_{t,T}$, a downward shift is indicated after the significant change point; If $K_T = -\min_{1\leqslant i<T} U_{t,T}$, an upward shift is convinced.

3.2.2. Shoreline extraction and morphological evolution

Muddy coast is highly turbid and fuzzy whose shoreline is difficult to catch (Liu et al., 2016). The normalized difference water index (NDWI) method (McFeeters, 1996), which has been widely used in separating the subaerial landscape from water bodies, is used here to extract the waterlines of Yellow River mouth. The radiation and atmospheric effects have been compensated by atmospheric correlation processes in the Landsat Ecosystem Disturbance Adaptive Processing System (LEDAPS) atmospheric correction tool (Masek et al., 2006). The NDWI method is described in Eq. (1), where Green and NIR represent the green light band and near-infrared band, corresponding to the second and fourth bands of TM and ETM + images, the third and the fifth bands of OLI satellite images.

$$NDWI = \frac{Green - NIR}{Green + NIR} \tag{1}$$

The waterlines extracted by the above described method are regarded as the shoreline in different period. Elevations of waterlines based on the local datum at Dongying Port (Fig. 1B) are converted into national elevation datum by adding 100 cm, being consistent with the elevation datum of subaqueous measurements. Combining the deltaic shoreline and field-observation data, we use Kriging technique in ArcGIS 10.3 to interpolate the subaqueous deltaic topography, with a cell resolution of 30 m × 30 m. The subaqueous morphological change (ΔV) in AYRM consists of common underwater topographic change ($\Delta V_{subaqueous}$) and sediment delivery for land building ($\Delta V_{subaerial}$). In Eq. (2), the elevation of subaerial delta is estimated the same as elevation of shoreline.

$$\Delta V = \Delta V_{subaqueous} + \Delta V_{subaerial} \tag{2}$$

In addition, to minimize the effect from the seasonal variability, the variation rate of morphologic change ($R\Delta_V$) and river delivery in adjacent years is accurately calculated to month as,

$$R_{\Delta V} = \frac{12 \times \Delta V}{month} \tag{3}$$

4. Results

4.1. The new regime of river discharge from Yellow river to the sea

Mann-Kendall (MK) test of annual variation trend indicates a significant decline in water discharge and sediment load delivered to the sea during 1950–2016, as recorded at Lijin station, the most seaward hydrological station, 109 km from the active river mouth (Fig. 2A and Table 2). In addition, the decline in sediment delivery has been greater than water discharge, due to the Z-value of the MK trend test in −6.55 and −7.30, respectively, with the Kendall slope of -6.53×10^8 m^3/yr and -0.21×10^8 t/yr. Pettitt test shows temporal abrupt change point occurred in 1985 of both time series in water and sediment discharge, which indicates a different time-series median occurring since 1986 compared to pre-1985 period (Fig. 2B and C). The average water discharge and sediment load shifted downward after the abrupt change point more than 63% and 76%. This change-point was probably associated with effective soil conservation practice in the middle reach and the closure of Longyangxia reservoir (1986) (Wang et al., 2007); Xiaolangdi reservoir, the most critical engineering project of Yellow River during 2000s, began to operate in 1999. Correspondingly, sediment delivery went on a decreasing trend with an average value of 1.20×10^8 t/yr, as a result of sediment retention behind dams. Whereas the average water discharging to the sea during 1986–1999 and 2000–2016 remained a relatively stable level with 150–155 × 10^8 m^3/yr by basin-scale flow regulation (Fig. 2D). The severe sediment starvation occurred in 2016 with the lowest level ever recorded at Lijin with only 10.6 Mt. The insufficient sediment delivery was less than 1% of 1950s-level, which represents the natural fluvial mode.

Despite the stepwise-decline in river input influenced by human impacts, the relationship between water and sediment discharge has greatly changed. Here we use the average annual incoming sediment coefficient (ξ_a), which reflects the relationship between incoming suspended sediment concentration (C_s) and water amount (Q_w):

$$\xi_a = \frac{C_s}{Q_w} = \frac{Q_s}{(Q_w)^2} \tag{4}$$

Between 1950 and 1985, the average incoming sediment coefficients at Huayuankou and Lijin were 0.021 and 0.024, respectively, which markedly increased to 0.030 and 0.066, after the closure of

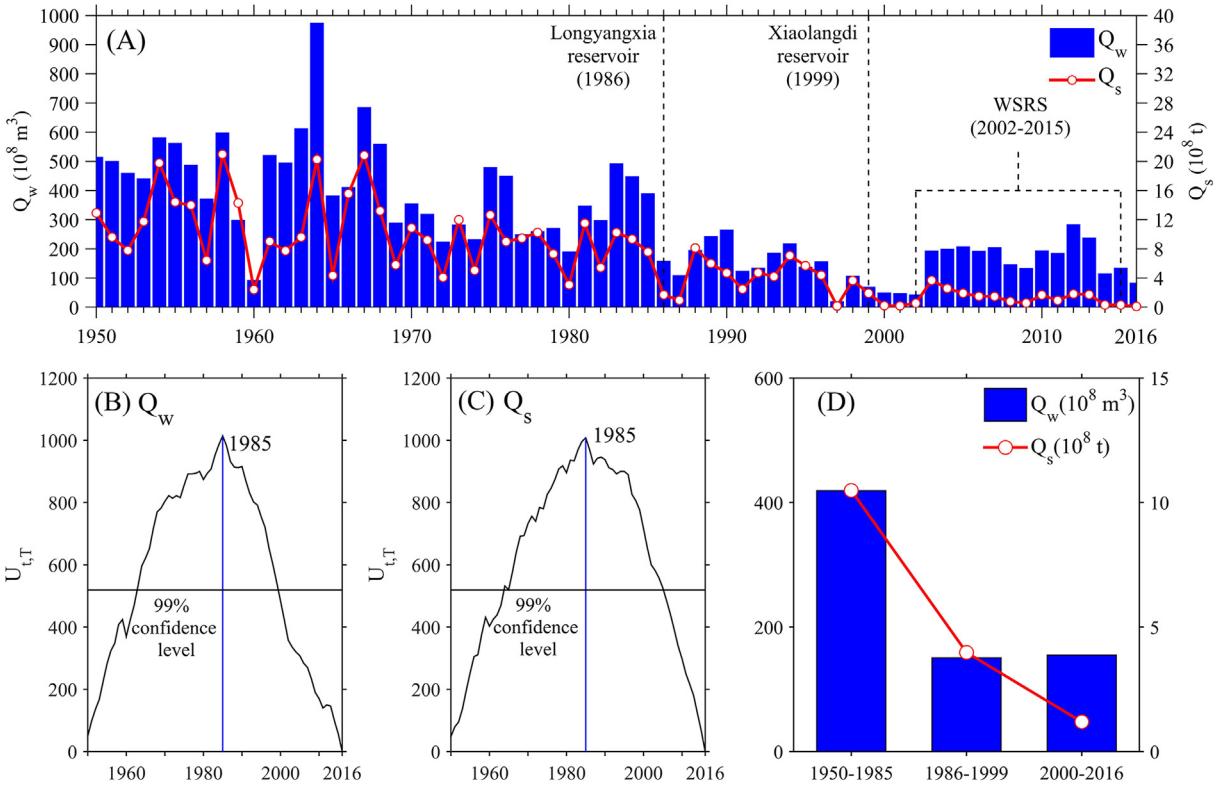

Fig. 2. (A) Temporal changes of annual water discharge (Q_w) and sediment load (Q_s) at Lijin, 1950–2016. The Sanmenxia and Xiaolangdi reservoir came into operation in 1986 and 1999, respectively. The 14-yr successive operation of WSRS was first interrupted in 2016 because of the absence of water discharge in the Yellow River basin; Detection of abrupt change point of (B) water discharge and (C) sediment load by Pettitt test; (D) Multistep-decline in river input during 1950–1985, 1986–1999 and 2000–2016. (For interpretation of the references to colour in this figure legend, the reader is referred to the web version of this article.)

Liujiaxia reservoir (Fig. 3A). It reflected the inconsistent relationship between water and sediment delivered to the lower reach and inevitably caused the decrease of sediment transport capacity and consequent heavy siltation in the lower reach riverbed. In addition, due to the drastic decline in water and sediment input, no-flow days appeared more frequently after 1986. In 1997, the length of riverbed drying up reached its peak level of 706 km and 226 no-flow days (Peng et al., 2010). To mitigate the excessive deposition state in the elevated riverbed in the lower reach, the Water-Sediment Regulation Scheme (WSRS) based at Xiaolangdi reservoir was designed to regulate river discharge and began its operation in 2002 (Wang et al., 2010b; Yu et al., 2013). The released flood water over a limited 20-day period effectively scoured the riverbed of the lower reach and deeply improved the environment of lower reach. Especially after 2005, the ξ_a at Huayuankou and Lijin both decreased lower than 0.014, the critical value for erosion-deposition trend in the lower reach suggested by Hu (2005), indicating the siltation in the lower reach has transformed directly to the net erosion state. On the other hand, linear regression relationship between water and sediment discharge shares similar trend between 1950 and 1985 and 1986–1999. After the closure of Xiaolangdi reservoir, the gradient of trend line after 1999 is significantly lower than the pre-1999 level, representing the relationship between water and sediment has completely changed into the harmonious, with drastic decline in annual suspended sediment concentration.

The fourteen years successive operation of WSRS had profound impacts on hydrological processes and source-to-sink cycles from the lower reach to the river mouth. The man-made flood peaks during WSRS has distinctively changed the distribution of river input through a year by delivering about 30% annual water discharge and 50% annual sediment load in limited ~20 days. In addition, the flow regulation successfully mitigated the excessive deposition state in the Xiaolangdi reservoir and the elevated riverbed of Yellow River lower reach, which made the riverbed downstream the Xiaolangdi becoming a new primary sediment source. Correspondingly, the median grain size of input increased to 25.8 μm in the early stage of the operation of the WSRS (2002–2007). However, the efficiency of lower reach scouring was slowed down since 2008, because most fine particles on the riverbed had been eroded and transported to the river mouth in the early years. The average median grain size decreased to 20.1 μm in the late stage of WSRS (2008–2015) (Fig. 4A). Fig. 4B shows a drastic decline in SSC peak value and significant seasonal migration since the completion of Xiaolangdi reservoir. The average SSC in flood season (July-October)

Table 2
Detection of trend and abrupt change point analysis using Man-Kendall test and Pettitt test.

Time-series	n	Man-Kendall test			Pettitt test			
		Z	Trend	*β*	K_T	*t*[a]	Shift	*P*[b]
Water discharge	67	−6.55	Decreasing	-6.53	1014	1985	Downward	0.00
Sediment load	67	−7.30	Decreasing	-0.21	1008	1985	Downward	0.00

[a] t represents the abrupt change temporal point.
[b] Both hydrologic time-series is significant at the significance level of 0.01.

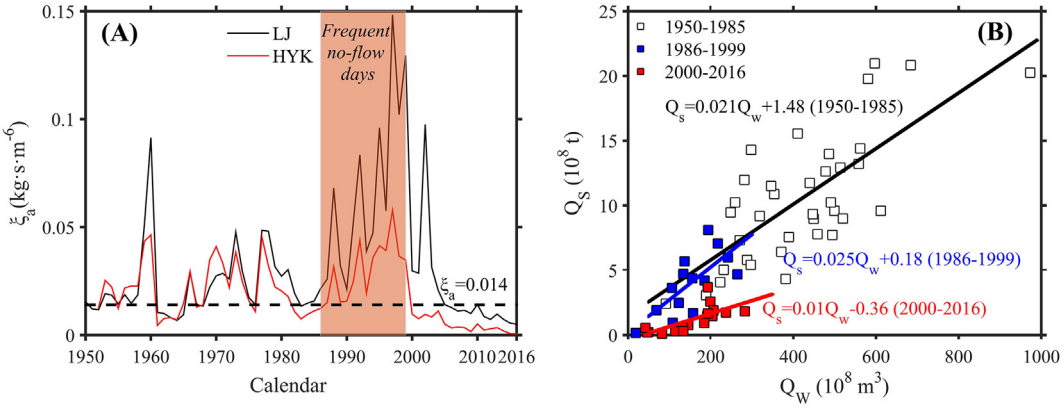

Fig. 3. Temporal changes of the relationship between water discharge (Q_w) and sediment load (Q_s). (A) Variability of incoming sediment coefficient (ξ_a) at Lijin (LJ) and Huayuankou (HYK) stations; (B) linear regression relationship between annual water discharge and sediment load in different periods.

reached 31.6 kg/m^3 in pre-1999, and migrated to its peak value with 9.1 kg/m^3 during June-July, when the WSRS frequently operated.

4.2. Erosion-deposition patterns in the active Yellow river mouth

To quantify the accurate morphological changes in AYRM, bathymetric survey data combined with DEM establishing is important. Thus, eight subaqueous data sets from field-observation, which were conducted in different years during 1996–2016, are transformed into the same projected coordinates UTM 50N with WGS84 datum. Based on the difference of DEM model in adjacent years, the erosion/accretion area and volume are calculated separately, which indicates the erosion-accretion pattern in AYRM (Fig. 5 and Table 3). According to the volume change rates and evolution processes, four major stages are generally divided by the initial implementation of WSRS (2002), mouth channel migration (2007) and the first interruption of WSRS (2016).

In the initial years of Qing 8 river mouth protruding prior to 2002, the subaqueous portion showed moderate accretion trend with 0.61 × 10^8 m^3/yr, and significant variance in evolution processes. We observed rapid deposition appearing with the depo-center located right in front of the river mouth during 1996–1998, severe erosion in 1998–2001 and accretion during 2001–2002 (Fig. 5A, B and C). The unexpected sedimentation percentage in 1996–1998 was 153%, presumably by the sufficient sediment source coming from southern old river mouth and the mouth channel riverbed as a result of the headward erosion. Additionally, the receiving basin of underwater topography provided an ideal place for sedimentation because of the initial steep profile. By contrast, the sediment supply decreased in 1998–2001, due to the integrated effect from low precipitation and dam impoundment of the Xiaolangdi reservoir. The AYRM experienced an average erosion rate of −0.13 m/yr, particularly for the mouth bar area where erosion-center is located (Table 3). At the beginning of the implementation of

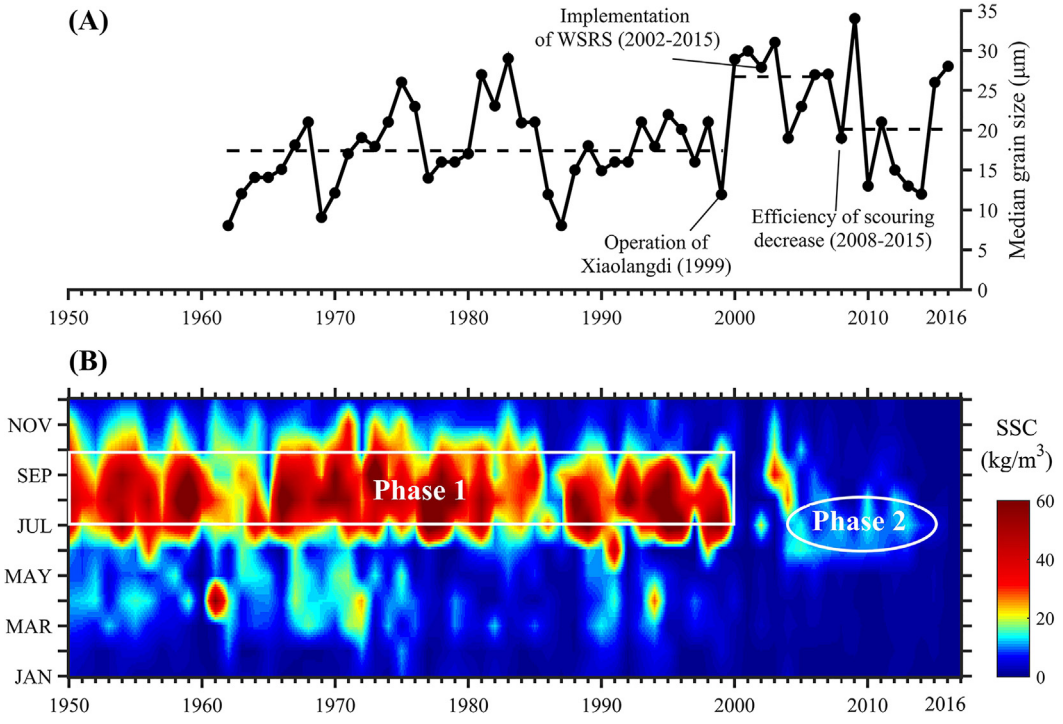

Fig. 4. Temporal change in median grain size of sediment delivery and monthly SSC. (A) Annual median grain size of suspended sediment at Lijin station. Operation of the Xiaolangdi reservoir and implementation of WSRS increase the median grain size of sediment input, but the efficiency of scouring of the lower reach by WSRS slowed down since 2007; (B) Distribution of monthly SSC at Lijin station in 1950–2016, showing drastic decline and seasonal migration of SSC from phase 1 (1950–1985, 1986–1999) to phase 2 (2000–2015).

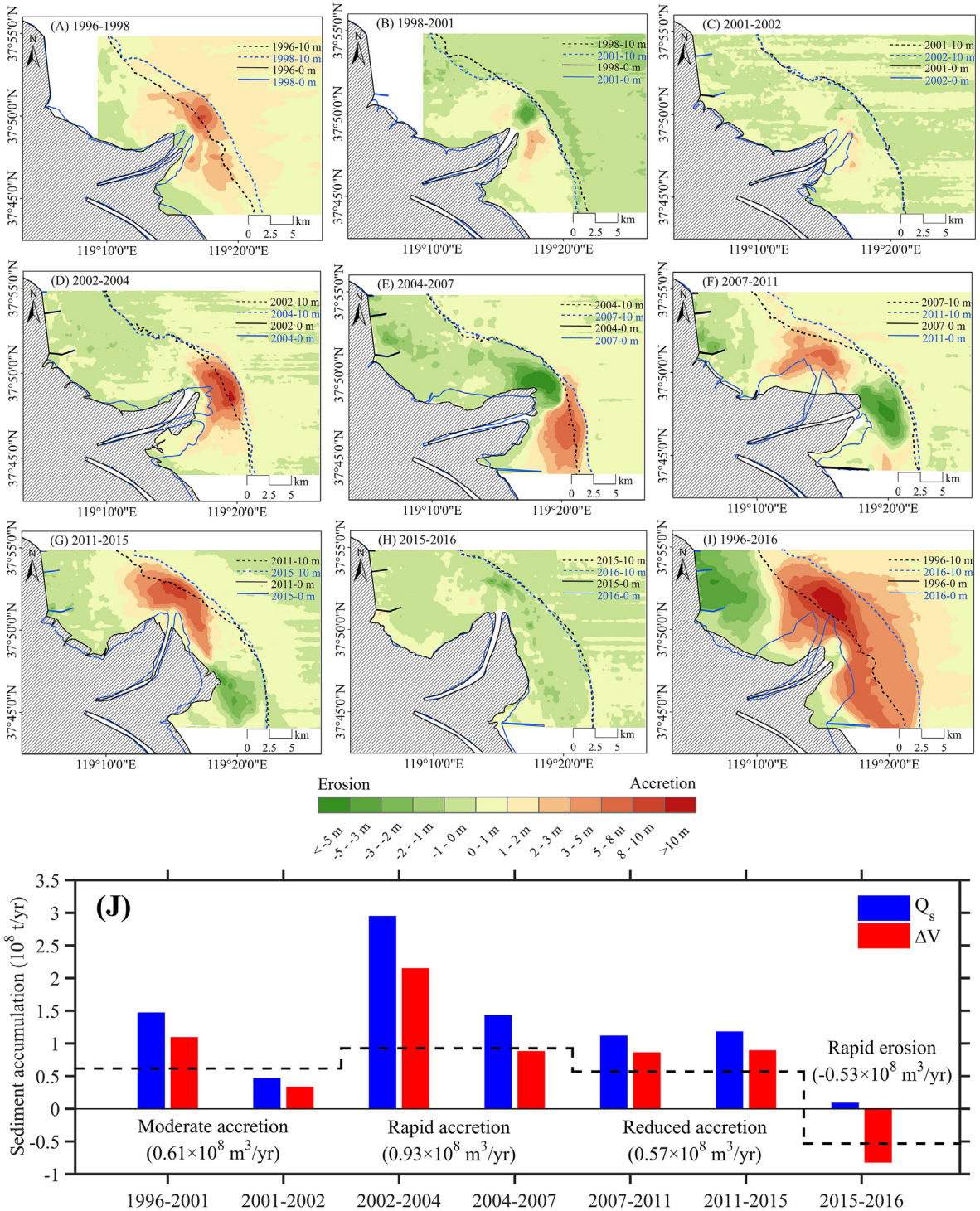

Fig. 5. Bathymetric changes in AYRM during (A) 1996–1998; (B) 1998–2001; (C) 2001–2002; (D) 2002–2004; (E) 2004–2007; (F) 2007–2011; (G) 2011–2015; (H) 2015–2016 and the entire 20-yr time span (I). The black and blue dash line indicated the shoreline and 10-m depth contour position of AYRM in adjacent years; (J) Erosion-accretion volume in AYRM (ΔV) and suspended sediment discharging to the sea (Q_s) during 1996–2016. The black dash line represents average volume change in AYRM in different period, indicating four different stages in AYRM variation. (For interpretation of the references to colour in this figure legend, the reader is referred to the web version of this article.)

WSRS, the considerable increase of sediment input induced rapid deposition during 2002–2007, with a rapid accretion trend at 0.93×10^8 m^3/yr. Approximately 61–73% of total sediment delivery deposited in AYRM during this stage, and most of them were found within 10-m water depth contour (Fig. 5D and E). As the river mouth shifted eastward during 2004–2007, the erosion-center and depo-center appeared simultaneously. We observed the erosion-center being around the left side of the sand spit near the river mouth where the water depth was shallower than 2 m, with an average erosion rate of −2.91 m/yr. Depo-center shifted to the location just seaward of the entrance bar at around 10-m depth contour, with an average vertical accretion rate of 3.14 m/yr. Sediment deposited in the mouth bar area before 2004 can be more easily suspended by winter waves and transported by shore-parallel currents, because of the sediment transport pathways changing with the

Table 3
Quantification test of erosion/accretion areas, volumes, net changes and depo-/erosion-center distribution in sub-areas AYRM and GDLZ. Positive values represent accretion and negative values represent erosion.

			1996–1998	1998–2001	2001–2002	2002–2004	2004–2007	2007–2011	2011–2015	2015–2016	1996–2016
		Sediment load (10^8 t)	4.92	2.17	0.54	5.89	3.81	4.64	4.91	0.1	27.0
		Time interval (month)	26	32	14	24	32	50	50	14	242
		Annual sediment load (10^8 t/yr)	2.27	0.82	0.46	2.95	1.43	1.11	1.18	0.09	1.34
AYRM	Area	Erosion (%)	5	78	49	24	24	13	32	65	2
		Accretion (%)	95	22	51	76	76	87	68	35	98
	Volume	Erosion (10^8 m^3)	−0.08	−2.14	−0.35	−0.17	−1.13	−0.89	−0.67	−0.83	−0.40
		Accretion (10^8 m^3)	5.00	0.64	0.60	2.97	2.65	3.22	3.08	0.21	11.93
	Net	Volume change (10^8 m^3)	4.91	−1.50	0.25	2.80	1.53	2.33	2.42	−0.62	11.90
		Volume change rate (10^8 m^3/yr)	2.27	−0.55	0.21	1.40	0.57	0.56	0.58	−0.53	0.59
		Vertical sedimentation rate (m/yr)	0.56	−0.13	0.05	0.34	0.15	0.14	0.16	−0.15	0.15
		Sedimentation percentage (%)[a,b]	153	–	71	73	61	77	75	–	68
	Center[c]	Deposition (m)	10.5	5.7	2.4	10.5	10.0	7.3	10.0	–	11.5
		Erosion (m)	–	2.5	–	–	0.25	0.90	0.52	1.17	–
GDLZ[d]	Area	Erosion (%)	93		63	81	94	64	66	77	94
		Accretion (%)	7		37	19	6	36	34	23	6
	Volume	Erosion (10^8 m^3)	−0.58		−0.09	−0.22	−0.45	−0.26	−0.17	−0.14	−1.63
		Accretion (10^8 m^3)	0.016		0.03	0.02	0.01	0.12	0.07	0.04	0.03
	Net	Volume change (10^8 m^3)	−0.56		−0.06	−0.20	−0.44	−0.14	−0.10	−0.10	−1.60
		Volume change rate (10^8 m^3/yr)	−0.12		−0.05	−0.10	−0.16	−0.03	−0.02	−0.09	−0.08
		Vertical erosion rate (m/yr)	−0.15		−0.06	−0.13	−0.20	−0.04	−0.03	−0.11	−0.10

[a] Sedimentation percentage refers to the proportion of sediment input that are finally deposition in the study area.
[b] Sediment bulk density is 1.533 g/cc, suggested by He et al. (2017).
[c] Locations of depo- and erosion-center are based on the underwater topography of the comparative previous year.
[d] Due to the lack of regional bathymetric dataset in GDLZ in 1998, the volume change is calculated from 1996 to 2001.

shift of river mouth at regional scale. During the flood season in 2007, the Yellow River mouth naturally shifted from eastward to northeastward, leaving previous river mouth abandoned due to the lack of sediment supply. During 2007–2011, depo- and erosion- centers interchanged the location with an average vertical rate of −1.53 m/yr in abandoned erosion-center and 1.49 m/yr in depo-center (Fig. 5F). This variation trend went on during 2011–2015, with a vertical erosion of erosion center 3.7 m and vertical accretion of depo-center over 10.0 m (Fig. 5G). Since the amount of sediment input decreased in 2007–2015, the deposition rate at this stage decreased to 0.57×10^8 m^3/yr. The 14-yr successive WSRS operation was first interrupted in 2016 because of the shortage of water discharge in the Yellow River basin. Meanwhile, the Yellow River sediment load reached the lowest level of 10.6 Mt in 2016. Consequently, approximately 65% of AYRM experienced erosion during 2015–2016 (Fig. 5H). Net erosion volume reached -0.62×10^8 m^3 and average vertical erosion rate in the study area exceeded 0.15 m (Table 3). It was the first time that AYRM experienced severe erosion since the implementation of WSRS.

Overall, the AYRM poses considerably varied trends as a result of inter-annual variability in sediment input. It is estimated that approximately 68% of overall sediment delivery contributed to subaerial building and subaqueous delta accretion in AYRM with net accretion rate 0.59×10^8 m^3/yr and an average vertical accretion of 0.15 m/yr (Fig. 5I). By comparing 20-yr net volume change rate of AYRM, we find the evolution of AYRM experienced four stages: i.e. moderate accretion (1996–2002) with 0.61×10^8 m^3/yr, rapid accretion (2002–2007) with 0.93×10^8 m^3/yr, reduced accretion (2007–2015) with 0.57×10^8 m^3/yr, and rapid erosion (2015–2016) with -0.53×10^8 m^3/yr (Fig. 5J).

4.3. Morphological change in Gudong littoral zone

The Yellow River delta is home to the local Shengli Oilfield, the second largest Oilfield in China (Fig. 6A). With sufficient supply of sediment in 1970s, the coastline at Gudong propagated seaward more than 5 km from 1976 to 1986. However, since 1987, the coastline was subject to erosion due to the reduction of sediment supply. An artificial coastal dike was first built to slow down the coastal erosion in 1987. Three groins were successively built along Gudong Dike in 2000s (Fig. 6B and C). Despite of the coastal defenses being built, the overall Gudong area continued to be in the state of erosion (Fig. 6D). During 1996–2016, more than 94% of GDLZ suffered from erosion, with an average erosion rate of 0.1 m/yr (Table 3). The inter-annual differences in erosion volume are believed to be determined by sediment delivery and the migration of river mouth. As the volume for coastal erosion has decreased after the natural migration of river mouth in 2007, erosion rate increased during 2015–2016 in comparison with that in 2007–2015, since there was a significant reduction of the sediment delivery. Bi et al. (2014) suggested a majority of suspended sediment from Yellow River mouth were trapped by the groins, where sediment transport pathway was intensively inhibited. In addition, waves driven by northeastward winter wind strengthened the sediment resuspension in GDLZ, which made GDLZ becoming an intensive erosion region, as the re-suspended sediment might be transported through parallel tidal current to AYRM or offshore.

Bathymetric cross-shore transect in GDLZ from 1976 to 2016 was also examined in this study to determine the temporal variation in subaqueous delta. The slope of delta front shallower than 5 m water depth in GDLZ shows gentle variation between 1976 and 1996, and falling from 0.64‰ to 0.39‰ during 1996–2016 (Fig. 6E). It should be noticed that the maximum erosion was distributed around the 2-m contour near Gudong Dike, where vertical erosion exceeded 5 m (Fig. 5I). By contrast, areas deeper than 5 m depth showed general accretion trend owing to the successive propagation of the active subaerial delta. The transect selected was crossing the mouth bar area with water depth less than 1 m (Fig. 6E black line).

5. Discussion

5.1. Factors controlling the deltaic variability under the new fluvial regime

5.1.1. Human activity-induced decline in river discharge

The delta morphologic processes are mainly dominated by terrestrial input, tides, wind waves, storm surges and sea-level conditions

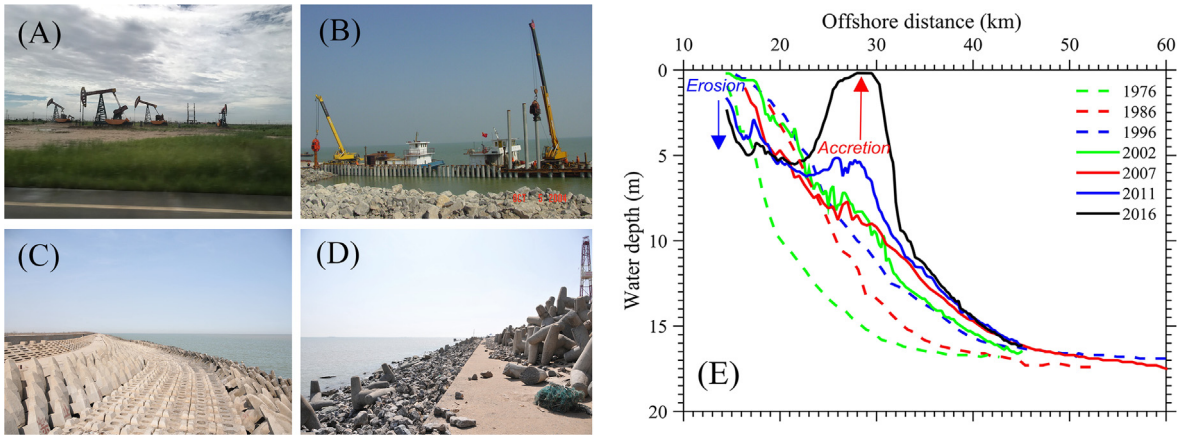

Fig. 6. Landscape of Gudong Oil Field and littoral zone. (A) Oil pumps in Gudong Oil Field, (B) Site observation in the construction of Gudong Dike, (C) Gudong Dike placed with twist blocks, (D) Serious damage in Gudong Dike, and (E) Selected cross-shore profile variation in GDLZ. Detailed location is in Fig. 1C.

(Blum and Roberts, 2009; Lamb et al., 2012; Hoitink et al., 2017). Adequate sediment input has direct and crucial impact on the building processes of fluvial-dominated deltaic system with relative weak tidal forcing and wave actions. Previous studies have revealed the inter-decadal variability of sediment accumulation rates in Qingshuigou abandoned river mouth was 5.77×10^8 m^3/yr during 1976–1985, 3.80×10^8 m^3/yr during 1986–1995 (Jiang et al., 2017), and further decreased to 0.61×10^8 m^3/yr since the river delivered by Qingbacha mouth channel in 1996. Similarly, the deposition zone over 6-m in vertical accretion during 1996–2016 has drastically shrank to 44.3 km^2, in contrast to an area of 183.06 km^2 in Qingshuigou old river mouth (Jiang et al., 2017). Moreover, from 1996 to 2016, AYRM deposit rate in four stages had strong correlation with the inter-annual variability of river input. The AYRM generally remained accretion under the condition of river input in the first three stages while showing erosion in 2016 with the absence of sediment supply. The littoral zone around 10-m contour relative to adjacent year is the most sensitive zone of accretion as the barrier effect of tidal shear front, which is the convergence of sedimentation. Numerical models show the river input largely influence the front intensity but has little influence to front locations (Qiao et al., 2008), which makes this convergence sedimentation center rather invariant in water depth.

Reduction in sediment supply from Yellow River to the sea is closely associated with human interference in the river basin. From the criterion suggested by Nilsson et al. (2005), the Yellow River belongs to strongly-affected river, since the dam storage capacity (56.3 km^3) and water consume (36.6 km^3) in the river basin have approached the mean annual discharge during 1950s-level (48 km^3) to the sea. Peng et al. (2010) indicated the relative contributions of human interference in the river basin and precipitation change to the multistep-decline of sediment load at Huayuankou based on the initial stage in 1950s. Sediment retention by dams together with soil conservation practice were responsible for 107% and 58% in sediment loss during 1960–1985 and 1986–1999 (Peng et al., 2010). The conservative estimates shows the sediment retention by soil conservation practice in the middle reach reaching 4.35×10^8 t/yr since 1996 (Gao et al., 2016). In addition, Sanmenxia together with Xiaolangdi reservoir accounted for 2.51×10^8 t/yr sediment retention during 2000–2016 (BCRS, 2000–2016), sand extraction in the lower reach for 0.2×10^8 t/yr for average (BYRS, 2006–2015). Thereafter, the direct human impacts have contributed to over 48% sediment loss from river catchment to river delta in total during 2000–2016. Other basin-scale human impacts and climate change include water consumption, reservoir storage dynamics, precipitation and evaporation variation, either of which will largely influence the water yield and in turn contributes to the sediment load change (Wang et al., 2015). Under this highly human-disturbed river system, it is convinced to believe the AYRM would be entering into an erosion stage, based on (1) more dams/reservoirs would be built in the Yellow River catchment, (2) high-level and relatively stable water-soil conservation practice, (3) a prediction of 74–122 mm sea level rise along the Yellow River coast in the next 30 years (BCSL, 2010), oil industry and aquaculture facilities in delta would accelerate this process (Higgins et al., 2013). Except for the estuaries of abandoned Yellow River delta lobe experiencing severe erosion as a result of the sediment absence, the AYRM is believed to be eroded under the new regime of terrestrial input in the next few years due to sediment starvation.

5.1.2. *Implementation of Water-Sediment Regulation Scheme*

The WSRS-induced coarser sediment with low SSC delivery has distinct impact on sediment dispersal and deposition pattern. Dong (1997) indicated 50% of sediment delivery contributed to the river mouth-rebuilt from 1964 to 1982. In comparison, our study finds a larger proportion with 68% of total sediment input deposition near the river mouth since river delivered by Qing 8 mouth channel. The reasons are multiple. Obviously, WSRS-induced floodwater effectively scour the riverbed of deltaic channel and change the heavy-deposition trend, which impels suspended sediment to transport to the coastal region. In addition, due to the low SSC, the buoyant hypopycnal plume replaced the hyperpcnal flow, which was frequently recognized in flood seasons near the Yellow River mouth during 1980s and 1990s. The river plume during flood season has a limited extent compared to pre-1999 periods (Wiseman et al., 1986; Wright et al., 1986, 1988, 1990; Wang et al., 2010a). Furthermore, sediment settling velocity (W) increases in square multiple with the sediment grain size (d) increases, according to Stokes formula. As a consequence, operation of WSRS changed the transport and deposition of silt-behavior. Coarser sediment delivered to the coastal oceans tended to deposit near the river mouth shallower than 10-m depth contour (Bi et al., 2014; Wu et al., 2017), which is evidenced by our study (Table 3).

Although floodwater is released from co-operation of upstream reservoirs in ~20 days, the event- scale WSRS plays a dominant role in reshaping evolutionary trends at longer timescale. Within annual scale, the protruding/retreating of active river mouth is the combined influence of short-term rapid seaward-advance (during WSRS) and long-term retreat by coastal dynamics. WSRS is short-term hydrological regulation processes, but providing sufficient sediment from the lower reach and reservoirs. Absence of WSRS can even cause erosion in active river mouth. As a majority of AYRM experienced the erosion with the first interruption of WSRS during 2015–2016 because the water discharge in the river catchment was extremely low.

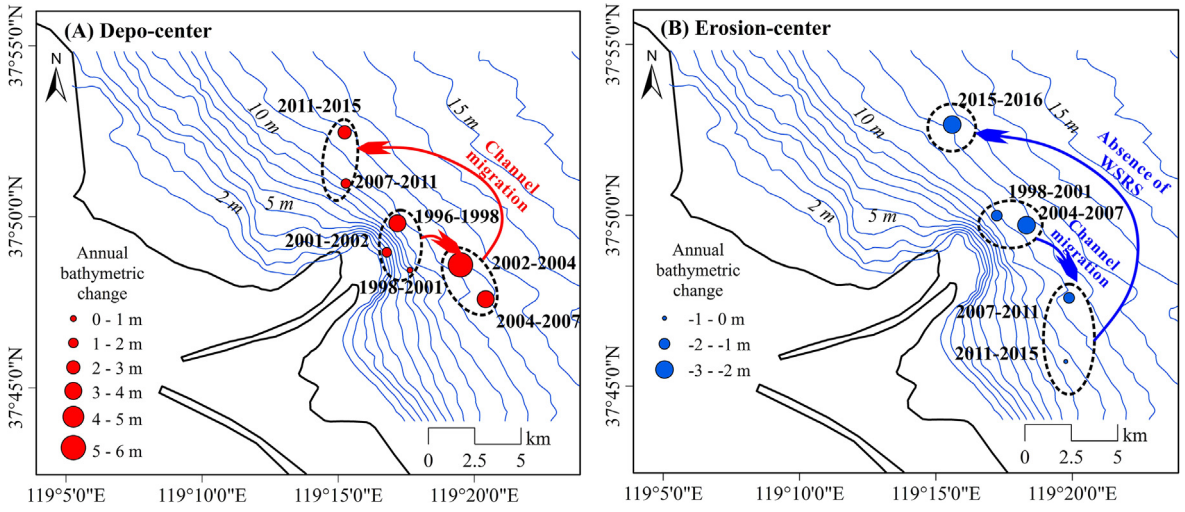

Fig. 7. Location variability of depo- and erosion-centers in AYRM. The red circle in (A) indicates the variation of accumulation depo-center and the blue circle in (B) represents the variation of erosion-center. The background underwater topography is based on bathymetric survey in 1996, implying for the relative plan location change of depo- and erosion-centers. (For interpretation of the references to colour in this figure legend, the reader is referred to the web version of this article.)

5.1.3. Migration pathway of mouth channel

In general, erosion and propagation rate of deltaic land is closely related to the switching depo-centers of rivers debouching to the sea (Fagherazzi et al., 2015), which is coincident with pathway changing of mouth channel, either naturally or through anthropogenic activities. The latest artificial channel diversion implemented in 1996 when channel migrated at Qing 8 section, causing subsequent evolution of sedimentation system. Wu et al. (2017) discovered the abandoned Qingshuigou sub-delta experienced significant shrink since the artificial diverted at Qing 8 section, as the absence of sediment supply. Consequently, the depo-center moved to the coastal zone near the active river mouth (Jiang et al., 2017). This erosion-deposition pattern indicates that the variation of spatial plan position in depo-center is strictly corresponded to the input mouth channel shifts. A particular interesting phenomenon appeared in 2007 again, when river mouth channel migrated from eastward to northeastward during the flood season, forming a new-born active river mouth. Fig. 7 shows the switching of erosion- and depo-center is highly corresponding to the channel migration in 2007. The depo-center moved to the vicinity of new river mouth and erosion-center appeared to the old, whose sedimentary system was eroded under the transport of tide- and wave-induced currents in the following years.

Unlike other bifurcation channels of large river deltas (for instance, Yangtze and Mississippi), whose sediment discharge partition in bifurcations largely influences depo-center locations, the active Yellow River delta forms its subaqueous deltaic system with no other than single main active mouth channel during a period. Therefore, the pathways migration of mouth channel has direct impact on sediment transport pathways and subaqueous erosion-deposition patterns. Although geomorphic variation of the whole active river mouth is largely influenced by the amount of sediment delivery, the shifts of local erosion-deposition trend influence the interactions between river flow and tidal dynamics from the point of morphodynamics, causing further migration in Qingbacha mouth channel and shoreline changes.

Under the environment of less flooding events, low river discharge and the protection of superelevated channel levees, the Yellow River deltaic channel is relatively stable, except for human-guiding avulsions since 1930s (Ganti et al., 2014). Most recently, competitive to the active mouth channel Qingbacha, Beicha has been considered as one of the potential mouth channel for the sustainability consideration of Gudong oilfield whose littoral zone has been seriously eroded in the past years (Fig. 1B). If Beicha becomes the pathway of mouth channel, the subaqueous sedimentation system is going to trigger a bigger transformation. Since the low river delivery and harmonious relationship between water and sediment, the deltaic mouth channel would be relatively stable. Hence, migration of channel perhaps would induce more direct evolution of subaqueous system compared to sediment supply at decadal or longer timescale.

5.2. Qualification of critical sediment discharge and implications for delta sustainability

Traditionally, deltaic morphological evolution is determined by relative strength of riverine input and coastal dynamics. Of all the influential factors, sediment delivery is the primary source and driving factor for the shaping of sedimentation system and delta morphology (Liu et al., 2014b; Kong et al., 2015b). Critical sediment delivery is the minimum requirement for erosion-accretion equilibrium, which has been calculated by a number of case studies through variation of subaerial area and long-term volume variability in subaqueous delta (Wang et al., 2006b; Cui and Li, 2011; Bi et al., 2014; Jiang et al., 2017; Fan et al., 2018b). However, few studies have concentrated on the critical sediment discharge of maintaining the AYRM. Based on sediment supply to the sea and accurate survey of underwater topography in AYRM, we build a linear regression model between volume change in active subaqueous delta (ΔV) and suspended sediment discharge (Q_s):

$$\Delta V_0 = 0.848 Q_s - 0.528, R^2 = 0.714, P = 0.008 \quad \text{(Trend 1)} \tag{5}$$

However, the correlation coefficient is not satisfying owing to the initial protruding of the river mouth before 2001 (blue dash circle in Fig. 8), which is rapidly-accretion in the initial deposition environment and sensitive to the abrupt decline in sediment discharge in 1999, 2000 and 2001. To avoid the error in fast-growing deltaic system and severe erosion drought years in initial stage, we take the 1996–2001 time series as a whole time series as,

$$\Delta V_1 = 0.606 Q_s - 0.251, R^2 = 0.900, P = 0.001 \quad \text{(Trend 2)} \tag{6}$$

When $\Delta V_0 = 0$, a threshold value of $Q_{s0} = 62.3$ Mt/yr and $Q_{s1} = 41.4$ Mt/yr, respectively, can achieve the Qing8 active subaqueous delta maintenance. The convincible result 41.4 Mt/yr–62.3 Mt/yr is highly-closed to the estimation through land area change from Bi et al. (2014) (50 Mt/yr). As for the sediment load passing Lijin station in 2016 is only 10.6 Mt, much lower than the critical sediment load calculated here and severe coastal erosion occurred in AYRM.

It is clear that the new riverine regime of Yellow River is dam-controlled, which is effective in reducing flood risk and managing water

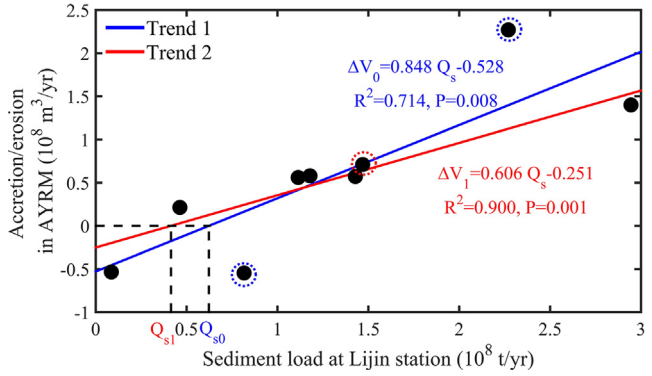

Fig. 8. Linear relationship between accretion/erosion volume in AYRM and sediment input. Trend 1 and Trend 2 indicate an annual sediment load threshold value 41.4 Mt/yr–62.3 Mt/yr can achieve the AYRM erosion-accretion balance.

resources. It is similar to other major rivers worldwide who have also witnessed the fluvial regime transforming from the natural to the highly human-regulated. However, sediment delivery has declined 98% in Nile, 69% in Mississippi, 66% in Yangtze and 99% in Yellow River from their natural modes, becoming the constraint for delta sustainability (Giosan et al., 2014). Our study shows not only the amount of sediment input, but water regulation program and mouth channel migration are important factors that dominating the erosion-accretion trends of active river mouth in different timescales. From the perspective of these factors, the integrated regulation strategies should consider the environmental implications both for the Yellow River lower reach and delta-building. WSRS has acted as a basin-scale water regulation program in mitigating infilling sediment in dams, flushing the lower reach and deltaic channel, providing substantial amount of sediment to the coastal ocean simultaneously. To meet the minimum sediment demands for sustaining AYRM, the water consumption and water discharge should be re-balanced on the basin-scale, aiming that more floodwater can be released by the integrated control of upstream dams. In this way, can the floodwater increase the sediment flushing amount and compensate the decrease of scouring efficiency in the lower reach. From the perspective of channel migration, the potential deltaic channel can be considered as sediment transport pathways for erosive coastal protection, like GDLZ. But future studies among scenario simulations between sediment flow and coastal dynamics should be carefully conducted before man-made avulsion projects.

5.3. Error analysis

The error from kriging interpolation technique utilized in this study is largely reduced if numerous topographic points are available (Yang et al., 2011a). The bathymetric data was from highly quality-controlled bathymetric surveys, hence is relatively accurate. The bathymetric contours are smooth and the interpolation result is convincible. It should be noticed that when calculating the sink direction of terrestrial sediment load, the volume change of subaerial land is underestimated. The elevation of new built-land is considered equal to the elevation of waterline (0 m). If the error of the elevation range of new born deltaic land is assumed to be 1 m, this will result in an error of the deviation of land-building of $0.51 \times 10^8\,m^3$ during 1996–2016, constituted approximately 2.89% of total sediment discharging to the sea during that period, which can be regarded as acceptable. We also ignored the influence of sea level rise to the volumetric change when comparing the tidal range and bathymetric change, since the sea level rise along Yellow River deltaic coast in the past two decades was only within 10 cm.

6. Conclusions

1. Yellow River discharge regime can be divided into three periods 1950–1985, 1986–1999 and 2000–2016, based on the abrupt change in river input reduction (1985) and construction of Xiaolangdi reservoir (1999). Water delivery was followed a dramatic decline in 1986 and remained a stable level since then, but sediment input was found successive declining in the three periods. The latest regime of riverine delivery featured the implementation of WSRS, which further altered the relationship between water and sediment discharge into the harmonious both in the lower reach of the Yellow River and to the sea.
2. The different segment in active YRSD present transverse evolution trends: accretion occurred in AYRM and erosion in GDLZ. The active river mouth since 1996 experienced four varied stages, namely: moderate accretion (1996–2002), rapid accretion (2002–2007), reduced accretion (2007–2015) and rapid erosion (2015–2016), which is closely related to sediment input variability at inter-annual scale. In contrast, GDLZ is convinced to experience severe erosion due to the absence of sediment supply and intensive sediment resuspension process driven by winter wind-waves.
3. The new regime of riverine delivery acts multiple timescales in shaping deltaic morphology. The inter-annual variability of river input has strong influence on the morphological change of AYRM. The man-altered water regulation program had critical impact on sediment source-to-sink transport and accumulation at event-scale. By low SSC and coarser sediment derived from the lower reach riverbed during WSRS, sediment accumulation is restricted within limited spatial range shallower than 10-m isobaths, and 68% sediment delivery deposited near the active river mouth with an average vertical accretion of 0.15 m/yr. At decadal timescale the pathway migration of mouth channels has directly impacted on subaqueous erosion-deposition patterns, exceeding the effect of sediment delivery to the deltaic system to some extent.
4. The interruption of 14-yr successive operation of WSRS in 2016 transformed the active river mouth from accretion to erosion for the first time. From the perspective of deltaic system, at least 41.4–62.3 Mt/yr of the sediment input is required to achieve the erosion-accretion balance of active river mouth. It is expected the overall Yellow River subaqueous deltaic system would remain the erosion state, as a result of intensified human impacts in the river basin. Additionally, our study reveals that basin-scale water regulation and channel migration projects can help sustain regional deltaic morphology.

Acknowledgements

This study was supported by the National Key Research and Development Program of China (No. 2017YFC0405503), the National Natural Science Foundation of China (NSFC) (No. U1706214) and the Open Research Fund (ORF) of State Key Laboratory of Estuarine and Coastal Research, ECNU (No. SKLEC-KF201503). We would like to acknowledge the hydrological dataset provided by the Yellow River Conservancy Commission, Ministry of Water Resources of China, and the open-source remote sensing data provided by the USGS. We would also thank the reviewers for their insightful and constructive comments.

References

Anthony, E.J., Brunier, G., Besset, M., Goichot, M., Dusssouillez, P., Nguyen, V.L., 2015. Linking rapid erosion of the Mekong River delta to human activities. Scientific Rep. 5, 14745.

Bi, N., Wang, H., Yang, Z., 2014. Recent changes in the erosion–accretion patterns of the active Huanghe (Yellow River) delta lobe caused by human activities. Cont. Shelf Res. 90, 70–78.

Bi, N., Yang, Z., Wang, H., Hu, B., Ji, Y., 2010. Sediment dispersion pattern off the present Huanghe (Yellow River) subdelta and its dynamic mechanism during normal river

discharge period. Estuar. Coast. Shelf Sci. 86 (3), 352–362.
Blum, M.D., Roberts, H.H., 2009. Drowning of the Mississippi Delta due to insufficient sediment supply and global sea-level rise. Nat. Geosci. 2 (7), 488–491.
Bulletin of China Sea Level (BCSL), 2010. State Oceanic Administration. http://data.mlr.gov.cn/hysj/201507/t20150720_1359795.htm.
Bulletin of Chinese River Sediment (BCRS), 2000-2016. Ministry of Water Resources Conservancy, Beijing, China. http://www.mwr.gov.cn/sj/tjgb/zghlnsgb/.
Bulletin of Yellow River Sediment (BYRS), 2006-2015. Yellow River Conservancy Commission, Zhengzhou, China. http://www.yellowriver.gov.cn/nishagonggao/.
Carriquiry, J.D., Sánchez, A., 1999. Sedimentation in the Colorado River delta and Upper Gulf of California after nearly a century of discharge loss. Mar. Geol. 158 (1), 125–145.
Chi, Y., Shi, H., Zheng, W., Sun, J., Fu, Z., 2018. Spatiotemporal characteristics and ecological effects of the human interference index of the Yellow River Delta in the last 30 years. Ecol. Ind. 89, 880–892.
Chu, Z.X., Sun, X.G., Zhai, S.K., Xu, K.H., 2006. Changing pattern of accretion/erosion of the modern Yellow River (Huanghe) subaerial delta, China: based on remote sensing images. Mar. Geol. 227 (1–2), 13–30.
Cui, B.-L., Li, X.-Y., 2011. Coastline change of the Yellow River estuary and its response to the sediment and runoff (1976–2005). Geomorphology 127 (1–2), 32–40.
Dai, S., Yang, S., Cai, A., 2008. Impacts of dams on the sediment flux of the Pearl River, southern China. Catena 76 (1), 36–43.
Dai, Z., Liu, J.T., Xiang, Y., 2015. Human interference in the water discharge of the Changjiang (Yangtze River), China. Hydrol. Sci. J. 60 (10), 1770–1782.
Dong, N., 1997. The deposit and diffuse of the Yellow River sediment into the sea. Ocean Eng. 15 (2), 59–64 (In Chinese with English Abstract).
Fagherazzi, S., Edmonds, D.A., Nardin, W., Leonardi, N., Canestrelli, A., Falcini, F., Jerolmack, D.L., Mariotti, G., Rowland, J.C., Slingerland, R.L., 2015. Dynamics of river mouth deposits. Rev. Geophys. 53 (3), 642–672.
Fan, Y., Chen, S., Zhao, B., Yu, S., Ji, H., Jiang, C., 2018a. Monitoring tidal flat dynamics affected by human activities along an eroded coast in the Yellow River Delta, China. Environ. Monit. Assess. 190 (7), 396.
Fan, Y., Chen, S., Zhao, B., Pan, S., Jiang, C., Ji, H., 2018b. Shoreline dynamics of the active Yellow River delta since the implementation of Water-Sediment Regulation Scheme: a remote-sensing and statistics-based approach. Estuar. Coast. Shelf Sci. 200, 406–419.
Ganti, V., Chu, Z., Lamb, M.P., Nittrouer, J.A., Parker, G., 2014. Testing morphodynamic controls on the location and frequency of river avulsions on fans versus deltas: Huanghe (Yellow River), China. Geophys. Res. Lett. 41 (22), 7882–7890.
Gao, J., Gao, Y., Yue, B., 2016. Analysis of Soil and Water Conservation Benefits of Yellow River Management in recent 70 Years. Yellow River 38 (12), 20–23 (In Chinese with English Abstract).
Giosan, L., Syvitski, J.P.M., Constantinescu, S., Day, J., 2014. Climate change: Protect the world's deltas. Nature 516, 31–33.
He, C., Li, X., Zuo, X., 2017. Analysis and research on sediment bulk density test in coastal area of Yellow River estuary. Water Resour. Dev. Manage. 4, 70–72 (In Chinese with English Abstract).
Higgins, S., Overeem, I., Tanaka, A., Syvitski, J.P.M., 2013. Land subsidence at aquaculture facilities in the Yellow River delta, China. Geophys. Res. Lett. 40 (15), 3898–3902.
Hoitink, A.J.F., Wang, Z.B., Vermeulen, B., Huismans, Y., Kästner, K., 2017. Tidal controls on river delta morphology. Nat. Geosci. 10 (9), 637–645.
Hu, C., 2005. Variation of flow and sediment and complicated response of channels in the Yellow River. The publishing company of science, Beijing.
Jiang, C., Pan, S., Chen, S., 2017. Recent morphological changes of the Yellow River (Huanghe) submerged delta: causes and environmental implications. Geomorphology 293, 93–107.
Kendall, M., 1975. Rank Correlation Measures. Charles Griffin, London, pp. 202p.
Kong, D., Miao, C., Borthwick, A.G.L., Duan, Q., Liu, H., Sun, Q., Ye, A., Di, Z., Gong, W., 2015a. Evolution of the Yellow River Delta and its relationship with runoff and sediment load from 1983 to 2011. J. Hydrol. 520, 157–167.
Kong, D., Miao, C., Wu, J., Jiang, L., Duan, Q., 2015b. Bi-objective analysis of water–sediment regulation for channel scouring and delta maintenance: A study of the lower Yellow River. Global Planet. Change 133, 27–34.
Kuenzer, C., Ottinger, M., Liu, G., Sun, B., Baumhauer, R., Dech, S., 2014. Earth observation-based coastal zone monitoring of the Yellow River Delta: Dynamics in China's second largest oil producing region over four decades. Appl. Geogr. 55, 92–107.
Lamb, M.P., Nittrouer, J.A., Mohrig, D., Shaw, J., 2012. Backwater and river plume controls on scour upstream of river mouths: Implications for fluvio-deltaic morphodynamics. J. Geophys. Res. Earth Surf. 117, F01002.
Li, G., Tang, Z., Yue, S., Zhuang, K., Wei, H., 2001. Sedimentation in the shear front off the Yellow River mouth. Cont. Shelf Res. 21 (6), 607–625.
Li, G., Wei, H., Yue, S., Cheng, Y., Han, Y., 1998. Sedimentation in the Yellow River delta, part II: suspended sediment dispersal and deposition on the subaqueous delta. Mar. Geol. 149 (1), 113–131.
Li, G., Zhuang, K., Wei, H., 2000. Sedimentation in the Yellow River delta. Part III. Seabed erosion and diapirism in the abandoned subaqueous delta lobe. Mar. Geol. 168 (1), 129–144.
Liu, F., Chen, S., Dong, P., Peng, J., 2012. Spatial and temporal variability of water discharge in the Yellow River Basin over the past 60 years. J. Geog. Sci. 22 (6), 1013–1033.
Liu, F., Yang, Q., Chen, S., Luo, Z., Yuan, F., Wang, R., 2014a. Temporal and spatial variability of sediment flux into the sea from the three largest rivers in China. J. Asian Earth Sci. 87, 102–115.
Liu, F., Yuan, L., Yang, Q., Qu, S., Xie, L., Cui, X., 2014b. Hydrological responses to the combined influence of diverse human activities in the Pearl River delta, China. Catena 113, 41–55.
Liu, X., Gao, Z., Ning, J., Yu, X., Zhang, Y., 2016. An improved method for mapping tidal flats based on remote sensing waterlines: A case study in the Bohai Rim, China. IEEE J. Sel. Top. Appl. Earth Obs. Remote Sens. 9 (11), 5123–5129.
Mann, H.B., 1945. Nonparametric tests against trend. Econometrica: J. Econometric Soc. 245–259.
Masek, J.G., Vermote, E.F., Saleous, N.E., Wolfe, R., Hall, F.G., Huemmrich, K.F., Gao, F., Kutler, J., Lim, T.K., 2006. A Landsat Surface Reflectance Dataset for North America, 1990–2000. IEEE Geosci. Remote Sens. Lett. 3 (1), 68–72.
McFeeters, S.K., 1996. The use of the Normalized Difference Water Index (NDWI) in the delineation of open water features. Int. J. Remote Sensing 17 (7), 1425–1432.
Miao, C., Ni, J., Borthwick, A.G.L., Yang, L., 2011. A preliminary estimate of human and natural contributions to the changes in water discharge and sediment load in the Yellow River. Global Planet. Change 76 (3–4), 196–205.
Milliman, J.D., Meade, R.H., 1983. World-wide delivery of river sediment to the oceans. J. Geol. 91 (1), 1–21.
Nilsson, C., Reidy, C.A., Dynesius, M., Revenga, C., 2005. Fragmentation and flow regulation of the world's large river systems. Science 308 (5720), 405–408.
Peng, J., Chen, S., Dong, P., 2010. Temporal variation of sediment load in the Yellow River basin, China, and its impacts on the lower reaches and the river delta. Catena 83 (2–3), 135–147.
Pettitt, A.N., 1979. A Non-Parametric Approach to the Change-Point Problem. J. Roy. Stat. Soc.: Ser. C (Appl. Stat.) 28 (2), 126–135.
Qiao, L.L., Bao, X.W., Wu, D.X., Wang, X.H., 2008. Numerical study of generation of the tidal shear front off the Yellow River mouth. Cont. Shelf Res. 28 (14), 1782–1790.
Ren, M.-E., Walker, J.H., 1998. Environmental consequences of human activity on the Yellow River and its delta, China. Phys. Geogr. 19 (5), 421–432.
Ren, R., Chen, S., Dong, P., Liu, F., 2011. Spatial and temporal variations in grain size of surface sediments in the littoral area of Yellow River Delta. J. Coastal Res. 28 (1A), 44–53.
Sanchez-Arcilla, A., Jimenez, J.A., Valdemoro, H.I., 1998. The Ebro Delta: morphodynamics and vulnerability. J. Coastal Res. 755–772.
Stanley, D.J., 1996. Nile delta: extreme case of sediment entrapment on a delta plain and consequent coastal land loss. Mar. Geol. 129 (3), 189–195.
Syvitski, J.P.M., Kettner, A.J., Overeem, I., Hutton, E.W.H., Hannon, M.K., Brakenridge, G.R., Day, J., Vörösmarty, C., Saito, Y., Giosan, L., Nicholls, R.J., 2009. Sinking deltas due to human activities. Nat. Geosci. 2 (10), 681–686.
Syvitski, J.P.M., Saito, Y., 2007. Morphodynamics of deltas under the influence of humans. Global Planet. Change 57 (3–4), 261–282.
Vörösmarty, C.J., Meybeck, M., Fekete, B., Sharma, K., Green, P., Syvitski, J.P.M., 2003. Anthropogenic sediment retention: major global impact from registered river impoundments. Global Planet. Change 39 (1–2), 169–190.
Walling, D.E., 2006. Human impact on land–ocean sediment transfer by the world's rivers. Geomorphology 79 (3–4), 192–216.
Wang, H., Bi, N., Wang, Y., Saito, Y., Yang, Z., 2010a. Tide-modulated hyperpycnal flows off the Huanghe (Yellow River) mouth, China. Earth Surface Processes Landforms 35 (11), 1315–1329.
Wang, H., Bi, N., Saito, Y., Wang, Y., Sun, X., Zhang, J., Yang, Z., 2010b. Recent changes in sediment delivery by the Huanghe (Yellow River) to the sea: causes and environmental implications in its estuary. J. Hydrol. 391 (3–4), 302–313.
Wang, H., Wu, X., Bi, N., Li, S., Yuan, P., Wang, A., Syvitski, J.P.M., Saito, Y., Yang, Z., Liu, S., Nittrouer, J., 2017a. Impacts of the dam-orientated water-sediment regulation scheme on the lower reaches and delta of the Yellow River (Huanghe): a review. Global Planet. Change 157, 93–113.
Wang, H., Yang, Z., Saito, Y., Liu, J.P., Sun, X., 2006a. Interannual and seasonal variation of the Huanghe (Yellow River) water discharge over the past 50 years: connections to impacts from ENSO events and dams. Global Planet. Change 50 (3–4), 212–225.
Wang, H., Yang, Z., Saito, Y., Liu, J.P., Sun, X., Wang, Y., 2007. Stepwise decreases of the Huanghe (Yellow River) sediment load (1950–2005): Impacts of climate change and human activities. Global Planet. Change 57 (3–4), 331–354.
Wang, S., Fu, B., Piao, S., Lü, Y., Ciais, P., Feng, X., Wang, Y., 2015. Reduced sediment transport in the Yellow River due to anthropogenic changes. Nat. Geosci. 9 (1), 38–41.
Wang, S., Hassan, M.A., Xie, X., 2006b. Relationship between suspended sediment load, channel geometry and land area increment in the Yellow River Delta. Catena 65 (3), 302–314.
Wang, Y., Liu, D., Lee, K., Dong, Z., Di, B., Wang, Y., Zhang, J., 2017b. Impact of Water-Sediment Regulation Scheme on seasonal and spatial variations of biogeochemical factors in the Yellow River estuary. Estuar. Coast. Shelf Sci. 198, 92–105.
Wiseman, W.J., Fan, Y.-B., Bornhold, B.D., Keller, G.H., Su, Z.-Q., Prior, D.B., Yu, Z.-X., Wright, L.D., Wang, F.-Q., Qian, Q-Y., 1986. Suspended sediment advection by tidal currents off the Huanghe (Yellow River) delta. Geo-Mar. Lett. 6 (2), 107–113.
Wright, L.D., Wiseman, W.J., Bornhold, B.D., Prior, D.B., Suhayda, J.N., Keller, G.H., Yang, Z.-S., Fan, Y.B., 1988. Marine dispersal and deposition of Yellow River silts by gravity-driven underflows. Nature 332 (6165), 629–632.
Wright, L.D., Wiseman, W.J., Yang, Z.S., Bornhold, B.D., Keller, G.H., Prior, D.B., Suhayda, J.N., 1990. Processes of marine dispersal and deposition of suspended silts off the modern mouth of the Huanghe (Yellow River). Cont. Shelf Res. 10 (1), 1–40.
Wright, L.D., Yang, Z.S., Bornhold, B.D., Keller, G.H., Prior, D.B., Wiseman, W.J., 1986. Hyperpycnal plumes and plume fronts over the Huanghe (Yellow River) delta front. Geo-Mar. Lett. 6 (2), 97–105.
Wu, X., Bi, N., Xu, J., Nittrouer, J.A., Yang, Z., Saito, Y., Wang, H., 2017. Stepwise morphological evolution of the active Yellow River (Huanghe) delta lobe (1976–2013): dominant roles of riverine discharge and sediment grain size. Geomorphology 292, 115–127.

Wu, X., Bi, N., Yuan, P., Li, S., Wang, H., 2015. Sediment dispersal and accumulation off the present Huanghe (Yellow River) delta as impacted by the Water-Sediment Regulation Scheme. Cont. Shelf Res. 111, 126–138.
Wu, Z.Y., Saito, Y., Zhao, D.N., Zhou, J.Q., Cao, Z.Y., Li, S.J., Shang, J.H., Liang, Y.Y., 2016. Impact of human activities on subaqueous topographic change in Lingding Bay of the Pearl River estuary, China, during 1955–2013. Scientific Rep. 6.
Xie, H., Li, D., Xiong, L., 2013. Exploring the ability of the Pettitt method for detecting change point by Monte Carlo simulation. Stoch. Env. Res. Risk Assess. 28 (7), 1643–1655.
Xing, G., Wang, H., Yang, Z.-S., Bi, N., 2016. Spatial and Temporal Variation in Erosion and Accumulation of the Subaqueous Yellow River Delta (1976–2004). J. Coastal Res. 74 (74), 32–47.
Xu, J., 2008. Response of land accretion of the Yellow River delta to global climate change and human activity. Quat. Int. 186 (1), 4–11.
Yang, S.L., Milliman, J.D., Li, P., Xu, K., 2011a. 50,000 dams later: Erosion of the Yangtze River and its delta. Global Planet. Change 75 (1–2), 14–20.
Yang, Z., Ji, Y., Bi, N., Lei, K., Wang, H., 2011b. Sediment transport off the Huanghe (Yellow River) delta and in the adjacent Bohai Sea in winter and seasonal comparison. Estuar. Coast. Shelf Sci. 93 (3), 173–181.
Yu, Y., Wang, H., Shi, X., Ran, X., Cui, T., Qiao, S., Liu, Y., 2013. New discharge regime of the Huanghe (Yellow River): causes and implications. Cont. Shelf Res. 69, 62–72.
Yue, T.X., Liu, J.Y., Jørgensen, S.E., Ye, Q.H., 2003. Landscape change detection of the newly created wetland in Yellow River Delta. Ecol. Model. 164 (1), 21–31.
Zhang, J., Huang, W.W., Shi, M.C., 1990. Huanghe (Yellow River) and its estuary: Sediment origin, transport and deposition. J. Hydrol. 120 (1), 203–223.
Zhang, S., Lu, X.X., Higgitt, D.L., Chen, C., Han, J., Sun, H., 2008. Recent changes of water discharge and sediment load in the Zhujiang (Pearl River) Basin, China. Global Planetary Change 60 (3–4), 365–380.
Zhang, W., Ruan, X., Zheng, J., Zhu, Y., Wu, H., 2010. Long-term change in tidal dynamics and its cause in the Pearl River Delta, China. Geomorphology 120 (3–4), 209–223.
Zhang, X., Wang, L., Fu, X., Li, H., Xu, C., 2017. Ecological vulnerability assessment based on PSSR in Yellow River Delta. J. Cleaner Prod. 167, 1106–1111.
Zhao, F.F., Xu, Z.X., Huang, J.X., Li, J.Y., 2008. Monotonic trend and abrupt changes for major climate variables in the headwater catchment of the Yellow River basin. Hydrol. Process. 22 (23), 4587–4599.
Zhao, G., Tian, P., Mu, X., Jiao, J., Wang, F., Gao, P., 2014. Quantifying the impact of climate variability and human activities on streamflow in the middle reaches of the Yellow River basin, China. J. Hydrol. 519, 387–398.
Zheng, S., Han, S., Tan, G., Xia, J., Wu, B., Wang, K., Edmonds, D.A., 2018. Morphological adjustment of the Qingshuigou channel on the Yellow River Delta and factors controlling its avulsion. Catena 166, 44–55.
Zhou, Y., Huang, H.Q., Nanson, G.C., Huang, C., Liu, G., 2015. Progradation of the Yellow (Huanghe) River delta in response to the implementation of a basin-scale water regulation program. Geomorphology 243, 65–74.